Influence of the magnetic field sweeping rate on magnetic transitions in synthetic ferrimagnets with perpendicular anisotropy

R. B Morgunov, E. I Kunitsyna, A. D Talantsev, O. V Koplak, T. Fache, Y. Lu, S Mangin

Influence of the magnetic field sweeping rate on magnetic transitions in synthetic ferrimagnets with perpendicular anisotropy

R.B. Morgunov[1, 2], E.I. Kunitsyna[1, 2], A.D. Talantsev[1, 2, 3], O.V. Koplak[1, 2], T.Fache[4], Y. Lu[4], S. Mangin[4]

[1] *Institute of Problems of Chemical Physics, 142432, Chernogolovka, Russia*

[2]*Tambov State Technical University, 392000, Tambov, Russia*

[3]*Department of Emerging Materials Science, DGIST, Daegu, 42988, Republic of Korea*

[4]*Institut Jean Lamour, UMR 7198 CNRS, Université de Lorraine, 54601, France*

[*]*E-mail: morgunov2005@yandex.ru*

Abstract

The evolution of the switching field between stable states in MgO/CoFeB/Ta/CoFeB/MgO/GaAs and Pt/Co/Ir/Co/Pt/Ta/SiO_2 synthetic ferrimagnets with perpendicular anisotropy as a function of the magnetic field sweeping rate (MFSR) 0.1 – 10^4 Oe/s has been studied. The most significant effect of the MFSR is an inversion of interstate transitions sequence. In the MgO/CoFeB/Ta/CoFeB/MgO/GaAs heterostructure, the increase of MFSR switches the dominant mechanism of magnetization reversal from propagation of domain walls to a nucleation of reversed magnetization areas. In Pt/Co/Ir/Co/Pt/Ta/ SiO_2, the MFSR affects the final domain state of the transition, starting from the initial antiparallel configuration of the synthetic ferrimagnet.

Key words: synthetic antiferromagnets, magnetic heterostructures, domain walls, perpendicular anisotropy, microwave magnetoresistance, magnetic relaxation, Kerr microscopy

I. INTRODUCTION

In the last ten years, magnetic relaxation of multilayered ferromagnetic heterostructures attracted a lot of interest due to its importance for the understanding of the magnetisation switching dynamics [1-3]. Magnetic relaxations in the MgO/CoFeB/Ta/CoFeB/MgO/GaAs [4] and Pt/Co/Ir/Co/Pt/Ta/Si [5] synthetic ferrimagnets with perpendicular magnetic anisotropy (PMA) have already been studied. The timescales of these relaxations range from few seconds to several hours. The duration of the magnetization reversal depends on the potency (expectation time) of the domain wall depinning and efficacy (kinetics) of nucleation of the reversed magnetization phase. These two mechanisms of the magnetic relaxation were combined in the Fatuzzo-Labrune model [6, 7], describing dynamics of magnetic relaxation in single ferromagnetic thin films, fully understood in the past years. Magnetic relaxation contributes to the shape of the hysteresis loop as well [8]. The shape of hysteresis loop and switching fields between the parallel and antiparallel states of synthetic antiferromagnets are strongly affected by the MFSR, when the duration of the loop recording is comparable to magnetic relaxation time. The latter depends on lateral size of heterostructure. If the lateral size is of a few nanometers and comparable with the thicknesses of the layers, the typical switching time ~ 1 ns is shorter by many orders of magnitude than the duration of a hysteresis loop recording by Kerr microscope (~ 1 s), vibration sample magnetometer (~ 1 min) and SQUID magnetometer (~ 1 h). Thus, the values of magnetization reversal parameters in nanosized heterostructures as nanopillars and nanodots are independent on the measurement technique used. On the opposite, heterostructures of a large lateral size (5 mm × 5 mm or larger) manifest long-lasting magnetic relaxation dynamics (~ 10^3–10^4 s), limited by the domain propagation time throughout the sample area [9, 10], and the duration of magnetization reversal can become comparable to magnetic hysteresis loop recording time. In that case, the observed value of the interstate transition field is expected to be strongly dependent on MFSR.

In general, synthetic antiferromagnets with two ferromagnetic layers of different thicknesses show four stable states, P^+, AP^+, AP^- and P^- (Figure 1a), corresponding to parallel and antiparallel mutual orientations of magnetizations in top and bottom layers (P and AP, respectively) and positive or negative sign of the net magnetic moment value (indicated by "+" or "-" sign). Magnetic field range, at which the interstate transition occurs, is dependent on the balance between the energy terms of synthetic antiferromagnet under applied magnetic field: magnetic energy of the layers, anisotropy energies, domain unpinning barriers and interlayer RKKY coupling. In this work, the thicknesses of the Co ferromagnetic layers and the Ir spacer layer in the Pt/Co/Ir/Co/Pt/Ta/SiO_2 structure were selected in a way, that the AP^+ to AP^- transition (synchronous reversals of the top and the bottom Co layers) and the AP^+ to P-

transition (reversal of the bottom Co layer only) are proceeding in overlapping field ranges. The MgO/CoFeB/Ta/CoFeB/MgO/GaAs structure was selected as a reference sample, where the transition fields do not overlap. This work is aimed at experimental analysis of MSFR effect on transition fields and transition sequence for the 'overlapping' case, and comparison of this effect with the conventional one in synthetic antiferromagnets without an overlap of transition fields.

II. EXPERIMENTAL

The MgO(2.5 nm)/CoFeB(1.1 nm)/Ta(0.75 nm)/CoFeB(0.8 nm)/MgO(2.5 nm)/Ta(5 nm) (Figure S1a) double ferromagnetic layer system was deposited on the undoped GaAs (001) substrate by magnetron sputtering. The EDX chemical analysis of the layers and TEM images of the cross-section of this heterostructure are presented in [11]. Continuous and homogeneous 3 × 3 mm^2 plate-shaped layer structures with perpendicular anisotropy were identified.

The multilayered structure Pt(3 nm)/Co(1.0 nm)/Ir(1.5nm)/Co(1.5 nm)/Pt(3 nm)/Ta(3nm)/ SiO_2 (Figure S1b) was prepared by deposition on the undoped Si/SiO_2 substrate of 0.4 x 4 x 5 mm^3 sizes by magnetron sputtering in 10^{-8} Torr vacuum. Iridium spacer allows one to predict the oscillating RKKY exchange interaction as a function of its thickness [12].

The recording of dynamic hysteresis loops and domain observation at room temperature (300 K) were performed by Durham Magneto-optics NanoMOKE3 magneto-optical Kerr effect measurement system, in polar MOKE measurement configuration. The domain imaging was performed at 2 Oe/s field sweep rate with an image scanning time of 0.5 s per frame, which was 10^2 – 10^4 times less, than the time of domain wall propagation through the microscope observation area.

Microwave non-resonant absorption was recorded by a Bruker ESP 300 X-band ESR spectrometer (microwave frequency was f_0 = 9.447 GHz, microwave power 6.3 mW, modulation frequency 100 kHz, modulation amplitude 10 Oe, quality factor Q ~ 4000). If the resistance of the sample is lower than resistance of the microwave circuit (R_C ~ 190 Ohm), absorbed microwave power P is proportional to sample resistance ρ and depends on magnetic field $P \sim \rho(H)$ [13-15]. Thus, in our experiments, the derivation of absorbed microwave power measured by modulation method was directly proportional to the derivation of specific resistance ρ of the sample $dP/dH \sim d(\rho(H))/dH$. Magnetic hysteresis loops were recorded by an MPMS 5XL Quantum Design superconducting quantum interference device (SQUID) magnetometer. The sweeping rate in this method was the slowest in comparison with two methods mentioned above.

This manuscript was accepted by Appl. Phys. Lett. Click here to see the version of record.

III. EXPERIMENTAL RESULTS AND DISCUSSION

A. CoFeB/Ta/CoFeB

The magnetic hysteresis loops recorded by MOKE technique at three different MFSR values in CoFeB bilayer (Sample **I**) at 300 K are presented in Figures 1 a,c,e. Parallel and antiparallel alignment of the magnetizations of the bottom layer (0.8 nm thickness) and top layer (1.1 nm) thickness result in four stable magnetic states P^+, P^-, AP^+ and AP^-. Transitions between the stable states result in three minor hysteresis loops: the central one and the two side ones, shifted from zero field by ~200 Oe due to the negative exchange coupling between both CoFeB layers [16]. The transition from AP^+ to AP^- state starts by nucleation of AP^- domains and their growth by propagation of AP^+/AP^- domain walls. Series of the microimages of one of the magnetic nuclei at MFSR = 2 Oe/s are presented in Figure 2a. The switching fields of the central (Figure S2) and side (Figure S3) hysteresis loops depend on the MFSR during loop recording. With an increase of the MFSR from 0.1 Oe/s (typical for SQUID magnetometer) to 10 kOe/s (typical for MOKE technique) the $AP^+ \rightarrow AP^-$ transition field grows 3 times, from 20 Oe to 60 Oe (Figure 3a). This growth of switching field with MSFR can be described in terms of energy balance for synthetic antiferromagnet.

In a single thin film, the dependence of the switching critical field, H_C, on the MFSR value dH/dt typically follows the logarithmic law [17,18]:

$$H_C(R) = H_f \ln(R) + \text{const} \quad (1)$$

H_f is fluctuation field, $R = dH/dt$ is MFSR.

To extend this equation for synthetic antiferromagnets, the interlayer coupling energy, magnetic energies of two layers and anisotropy energies should be taken into account.

For $AP^+ \rightarrow AP^-$ transition

$$H_C = H_f \ln\left(\frac{R}{R_0}\right) + \frac{K_A}{2M_S}\frac{h_2+h_1}{h_2-h_1} \quad (2),$$

$$H_f = \frac{kT}{2M_S V_A}\frac{h_2+h_1}{h_2-h_1} \quad (3),$$

$$R_0 = \frac{f_0 kT}{M_S V_A}\frac{h_2+h_1}{h_2-h_1} \quad (4),$$

where K_A – anisotropy constant, V_A – activation volume, M_S – saturation magnetization (K_A and M_S values were supposed to be similar for top and bottom layers of synthetic antiferromagnet), h_1 and h_2 – thicknesses of top and bottom layers, respectively, f_0 – attempt frequency (Arrhenius factor) of domain nucleation. The interlayer coupling energy is not present in Eq. (2-4), as the $AP^+ \rightarrow AP^-$ transition proceeds between two antiparallel states, and, therefore, does not change the sign of interlayer coupling. However, the switching field depends

This manuscript was accepted by Appl. Phys. Lett. Click here to see the version of record.

on interlayer coupling energy for $P^+ \rightarrow AP^+$ and $AP^- \rightarrow P^-$ transitions, when the mutual orientation of magnetizations in top and bottom layers changes from collinear to opposite and vice versa (See Appendix I in Supporting section).

The derivation of these equations, and the formulas for other transitions in the synthetic antiferromagnet are given in Appendix I Supporting section. The Eq. (3) for a fluctuation field in a bilayer system is similar to the one for single layer thin films [19],

$$H_f = kT/(2V_A M_S) \qquad (5)$$

with an exception of $(h_2 + h_1) / (h_2 - h_1)$ term. The physical meaning of this term is that for same temperature and activation volume, the fluctuation field in a bilayer is much larger, than in a single layer thin film. The H_f value depends on mechanism of the domain wall pinning and is sensitive to the "strong" or "weak" pinning cases [20, 21]. Thus, the H_f parameter characterizes thermal stability of the material, being dependent on the ratio between the energy of the reversal magnetization phase nucleation and the energy of the domain walls pinning by structural defects. Since the thicknesses of the magnetic layers in our samples (0.8 nm and 1.1 nm) are of a few lattice parameters (0.4 nm), any defect of crystalline structure corresponds to a local change of the film thickness by 20-30%. For that reason, the fluctuation field H_f is comparable to the coercive field H_C (Table 1 in Supporting section) and can be changed by few times in contrast to the bulk sample or thick (> 10 nm) films, where change of the MFSR by few orders of value causes change in H_f by few percent. Thus, in the thin films, results of measurements of the fluctuation field strongly depend on the method of measurement (in SQUID MFSR = 0.1 Oe/s, in FMR MFSR = 0.2 – 20 Oe/s (Figure S4), in MOKE microscope MFSR = 10 kOe/s).

The $H_C(\ln R)$ dependence has a kink at $R \sim 500$ Oe/s (Figure 3a). This kink cannot be explained by the change of the sign of the derivative of domain wall velocity in magnetic field close to the Walker limit [22, 23]. A more realistic explanation of the kink can be proposed on the basis of consideration of the competition between two ways of transitions from AP^+ to AP^- state: by nucleation of the magnetization reversal phase and propagation of the domain walls. In this mode the number of nuclei becomes dependent on the external magnetic field before full magnetization reversal of the film is realized by the growth of nuclei. Thus, the activation volume and fluctuation field in high MFSR modes are controlled by both the nucleation field and the depinning field (see Figure S5 in Supporting section).

B. Pt/Co/Ir/Co/Pt/Ta/ SiO_2 heterostructure

An evolution of magnetic hysteresis loop with MFSR for the Pt/Co/Ir/Co/Pt/Ta/ SiO_2 structure (sample **II)**, is presented in Figure 1 b,d,f. In addition to the shift of transition fields, an increase of MFSR results in the inversion of interstate transition sequence. At slow field sweep rates (below 0.01 kOe/s) the switching from AP^+ state to P^- state proceeds via AP^- state as two

This manuscript was accepted by Appl. Phys. Lett. Click here to see the version of record.

separate transitions: i) $AP^+ \rightarrow AP^-$ – synchronous propagation of AP^+/AP^- domain wall in top and bottom Co layers at 470 – 520 Oe field range, and ii) $AP^- \rightarrow P^-$ – nucleation of domains in top Co layer, at 720 – 750 Oe field range. With an increase of MFSR, it is expected, that $AP^+ \rightarrow AP^-$ transition field will increase, until it reaches the $AP^- \rightarrow P^-$ transition field (~750 Oe) and the AP^- state is no more dwelled. However, a different process is experimentally observed. The $AP^+ \rightarrow AP^-$ transition field does not reach the $AP^- \rightarrow P^-$ transition field. Instead, at ~ 550 Oe a domain nucleation in bottom layer, resulting in the direct transition from AP^+ to P^- state, starts to proceed together with the $AP^+ \rightarrow AP^-$ one. When the MFSR is in a range of 0.02 kOe/s – 0.45 kOe/s, these two processes are occurring together and competitively, leading to multi-domain stable magnetic state (AP^-; P^-), laying in-between AP^- and P^- (Figure 1d).

A series of the MOKE images recorded in intermediate MFSR is shown in Figure 2b. Three types of areas can be distinguished in these images: dark areas correspond to the AP^+ state, the areas of the intermediate brightness correspond to the AP^- state, and light areas correspond to the P^- state. When this transition is completed (Figure 2b, last image), domains of two states AP^- and P^- coexist and this (AP^-; P^-) state is stable in 550 Oe – 750 Oe field range. The proportion between the areas, occupied by of AP^- and P^- domains, was found to be dependent on MFSR (Figure S6 Supporting information). When the field reaches 750 Oe, those areas, which are in AP^- state, are switching to P^- state, until all the areas of the film are switched to P^- state.

At high MFSR values (> 0.5 kOe/s), the transition in 750 Oe disappears (Figure 1f) and the reversal from AP^+ to P^- state becomes fully completed at lower magnetic field, ~600 Oe, corresponding to the nucleation of magnetic domains in the bottom Co layer. It means that at high MFSR the reversal from AP^+ to P^- is localized in the bottom Co layer only. No formation of domain nuclei in the top Co layer occurs at high MFSR. On the opposite, at low MFSR values, due to AP^+ to AP^- preceding process, the domain nucleation occurs in the top Co layer and does not happen in the bottom Co layer. Thus, an increase of MFSR results in relocalization of domain nucleation process from the top to the bottom Co layer, by suppression of propagation of AP^+/AP^- domain walls. The evidence of this relocalization are: i) appearance of direct $AP^+ \rightarrow P^-$ process, corresponding to domain nucleation in bottom Co layer, at intermediate MFSR, and ii) disappearance of transition at 750 Oe, corresponding to domain nucleation in the top Co layer, at high MFSR.

Dynamics of the AP^- and P^- domain nucleation and propagation is summarized in Figure S5 b of Supporting section for three ranges of the MFSR: slow mode (< 0.01 kOe/s), intermediate mode (0.02 kOe/s – 0.45 kOe/s) and fast mode (> 0.5 kOe/s). For the transitions, starting from the AP^+ state, the dependences of switching fields on MFSR are presented in the

Figure 3b. The fluctuation field and the activation volume, extracted by linear approximations of the straight parts of these dependences by formula (1), are presented in Table 1 of Supporting section. These values are close to the ones obtained in $SmCo_5/Fe/SmCo_5$ trilayers [3] and Co/Pt multilayer structures [24]. The $H_C(dH/dt)$ dependences abruptly change slope at critical dH/dt value in CoFeB sample, as well as in the Pt/Co sample. However, the origins of these features are different in Pt/Co and CoFeB synthetic ferrimagnets. In the CoFeB based heterostructures, the slope increases due to the progressive involvement of domain nucleation process with the increase of MFSR. In contrast to CoFeB synthetic ferrimagnets, in the Pt/Co samples the slope of $H_C(dH/dt)$ decreases, and it is caused by migration of the final magnetization state. At low MFSR values the $AP^+ \rightarrow AP^-$ transition takes place, while at high MFSR values the $AP^+ \rightarrow P^-$ transition occurs. Different slopes of the dependence of switching field H_C on the sweeping rate $R = dH/dt$ in logarithmic coordinates (H_C; ln(R)) (Figure 3b) indicates the difference between the fluctuation fields and activation volumes corresponding to the $AP^+ \rightarrow AP^-$ and $AP^+ \rightarrow P^-$ transitions most probably due to different heights of the activation barriers of these transitions. The $AP^+ \rightarrow P^-$ transition corresponds to the magnetization reversal of just one of the ferromagnetic layers. Thus, the realization of the $AP^+ \rightarrow P^-$ transition requires overcoming the barrier E_1 corresponding to the single layer, while the $AP^+ \rightarrow AP^-$ transition corresponds to magnetization reversal of the both layers requiring to overcome sum of the activation energies $E_1 + E_2$ of the both ferromagnetic layers.

IV. CONCLUSIONS

In multilayered synthetic ferrimagnets Pt/Co/Ir/Co/Pt and CoFeB/Ta/CoFeB with perpendicular anisotropy, magnetic field sweeping rate dependence of the switching field between different stable states has been investigated. The increase of the sweeping rate on 5 orders of magnitude from 0.1 Oe/s up to 10 kOe/s changes the $AP^+ \rightarrow AP^-$ switching field in CoFeB/Ta/CoFeB by a factor of 3 (from 20 Oe till 60 Oe). More interestingly, in a Pt/Co/Ir/Co/Pt heterostructure, the sequence of the transitions between stable states can be changed by controlling the sweeping rate of the magnetic field.

Two mechanisms could be proposed to explain those behaviors. In CoFeB/Ta/CoFeB by modifying the sweeping rate the magnetisation reversal changes from domain wall propagation to nucleation, dominating at high sweeping rate. In the Pt/Co/Ir/Co/Pt structure, an increase of the magnetic sweeping rate changes the type of switching from $AP^+ \rightarrow AP^-$ and $AP^- \rightarrow P^-$ transitions. Simultaneous contributions of the $AP^+ \rightarrow AP^-$ and $AP^+ \rightarrow P^-$ transitions to magnetization reversal results in a stable multi-domain state of the heterostructure, with coexisting domains of AP^- and P^- states.

An increase of MFSR results in the relocalization of domain nucleation process from the top to the bottom Co layer, by suppression of the propagation of AP^{+}/AP^{-} domain walls. The evidences of this relocalization are: i) appearance of a direct $AP^{+} \rightarrow P^{-}$ process, corresponding to domain nucleation in the bottom Co layer, at intermediate MFSR, and ii) disappearance of transition at 750 Oe, corresponding to domains nucleation in the top Co layer, at high MFSR.

SUPLEMENTARY MATERIAL

See Supplementary material for the structure of two samples, complete ESR and MOKE data of the samples, sketch of the nucleation for different MFSR and activation volumes of the transitions.

ACKNOWLEDGEMENTS

The R.M., E.K, A.T. and O.K were supported by Ministry of Education and Science of Russian Federation (grant 3.1992.2017/4.6). A.T. was supported by the R&D program of MOTIE/KEIT (10064089, Development of low power current sensor and module for automotive with 0.1% precision), and the DGIST R&D Program of the Ministry of Science, ICT and Future Planning (19-BT-02). S.M., T.F. and Y.L. were supported by the ANR-NSF Project, ANR-13-IS04-0008-01, COMAG, ANR- 15-CE24-0009 UMAMI and by the ANR-Labcom Project LSTNM, by the Institut Carnot ICEEL for the project “Optic-switch” and Matelas and by the French PIA project “Lorraine Université d’Excellence”, reference ANR-15IDEX-04-LUE. Experiments were performed using equipment from the TUBE Davm, funded by FEDER (EU), ANR, Région Grand Est and Métropole Grand Nancy.

References

[1] J. E. Davies, O. Hellwig, E. E. Fullerton, K. Liu. Phys. Rev. B **77**, 014421 (2008).

[2] H. Liu, D. Bedau, J. Z. Sun, S. Mangin, E. E. Fullerton, J. A. Katine, A. D. Kent. Journal of Magnetism and Magnetic Materials **358–359**, 233 (2014).

[3] S. J. Collocott, V. Neu. J. Phys. D: Appl. Phys. **45**, 035002 (2012).

[4] R. Morgunov, Y. Lu, M. Lavanant, T. Fache, X. Deveaux, S. Migot, O. Koplak, A. Talantsev, S. Mangin. Physical Review B **96**, 054421 (2017).

[5] A Talantsev, Y Lu, T Fache, M Lavanant, A Hamadeh, A Aristov, O Koplak, R Morgunov, S Mangin. Journal of Physics: Condensed Matter **30**, 135804 (2018).

[6] M. Labrune, S. Andrieu, F. Rio, P. Bernstein. Time dependence of the magnetizaton process of Re-TM alloys, J. Magn. Magn. Mater. **80**, 211 (1989).

[7] E. Fatuzzo, Theoretical considerations on the switching transient in ferroelectrics, Phys. Rev. **127**, 1999 (1962).

[8] Xiao Xu, Takumi Kihara, Masashi Tokunaga, Akira Matsuo, Wataru Ito, Rie Y. Umetsu, Koichi Kindo, Ryosuke Kainuma. J. Appl. Phys. Lett. **103**, 122406 (2013).

[9] R. B. Morgunov, G. L. L'vova, A. D. Talantsev, O. V. Koplak, T. Fache, S. Mangin. J. Magn. Magn. Mater. **459**, 33 (2018).

[10] T. Fache, H. S. Tarazona, J. Liu, G. L'vova, M. J. Applegate, J. C. Rojas-Sanchez, S. Petit-Watelot, C. V. Landauro, J. Quispe-Marcatoma, R. Morgunov, C. H. W. Barnes, S. Mangin. Physical Review B **98**, 064410 (2018).

[11] S. H. Liang, T. T. Zhang, P. Barate, J. Frougier, M. Vidal, P. Renucci, B. Xu, H. Jaffrès, J. M. George, X. Devaux, M. Hehn, X. Marie, S. Mangin, H. X. Yang, A. Hallal, M. Chshiev, T. Amand, H. F. Liu, D. P. Liu, X. F. Han et al., Phys. Rev. B **90**, 085310 (2014).

[12] Y. Luo, M. Moske, and K. Samwer, Europhys. Lett. **42**, 565 (1998).

[13] R. Morgunov, G. L'vova, A. Talantsev, O. Koplak, S. Petit-Watelot, X. Devaux, S. Migot, Y. Lu, and S. Mangin. Appl. Phys. Lett. **110**, 212403 (2017);

[14] A. I. Veinger, A. G. Zabrodskii, and T. V. Tisnek, Phys. Status Solidi B **230**, 107 (2002).

[15] R. Morgunov, M. Farle, M. Passacantando, L. Ottaviano, and O. Kazakova, Phys. Rev. B **78**, 045206 (2008).

[16] O. Koplak, A. Talantsev, Y. Lu, A. Hamadeh, P. Pirro, T. Hauet, R. Morgunov, S. Mangin. J. Magn. Magn. Mat. **433**, 91 (2017).

[17] P. Bruno, G. Bayreuther, P. Beauvillain, C. Chappert, G. Lugert, D. Renard, J.P. Renard, J. Seiden. J. Appl. Phys. **68**, 5759 (1990).

[18] M. El-Hilo, A.M. de Witte, K. O'Grady and R.W. Chantrell, J.Magn.Magn.Mat.

117, L307 (1992).

[19] E. P. Wohlfarth. J. Phys. F: Met. Phys. **14** L155 (1984).

[20] P. Gaunt. Phil. Mag. B **48**, 261 (1983).

[21] P. Gaunt. J. Appl. Phys. **59**, 4129 (1986).

[22] N. L. Schryer, L. R. Walker. J. Appl. Phys. **45**, 5406 (1974).

[23] T. Devolder, P.-H. Ducrot, J.-P. Adam, I. Barisic, N. Vernier, Joo-Von Kim, B. Ockert, D. Ravelosona. J. Appl. Phys. Lett. **102**, 022407 (2013).

[24] Yoon-Chul Cho, Sug-Bong Choe, Sung-Chul Shin. J. Appl. Phys. Lett. **80**, 452 (2002).

Captions for figures

Figure 1. MOKE hysteresis loops of Sample **I** (a, c, e) and Sample **II** (b, d, f), recorded at T = 300 K at 0.01 kOe/s, 0.08 kOe/s and 0.5 kOe/s magnetic field sweep rates.

Figure 2. MOKE images of domains, corresponding to $AP^{+} \rightarrow AP^{-}$ transition field range, in Sample **I** (MgO/CoFeB/Ta/CoFeB/MgO) (a) and Sample **II** (Pt/Co/Ta/Co/Pt) (b), recorded at T = 300 K at 2 Oe/s magnetic field sweep rate.

Figure 3. The dependence of transition field on magnetic field sweep rate (semi-logarithmic scale), for Sample **I** (MgO/CoFeB/Ta/CoFeB/MgO) (a) and Sample **II** (Pt/Co/Ir/Co/Pt) (b). Solid lines are linear approximations.

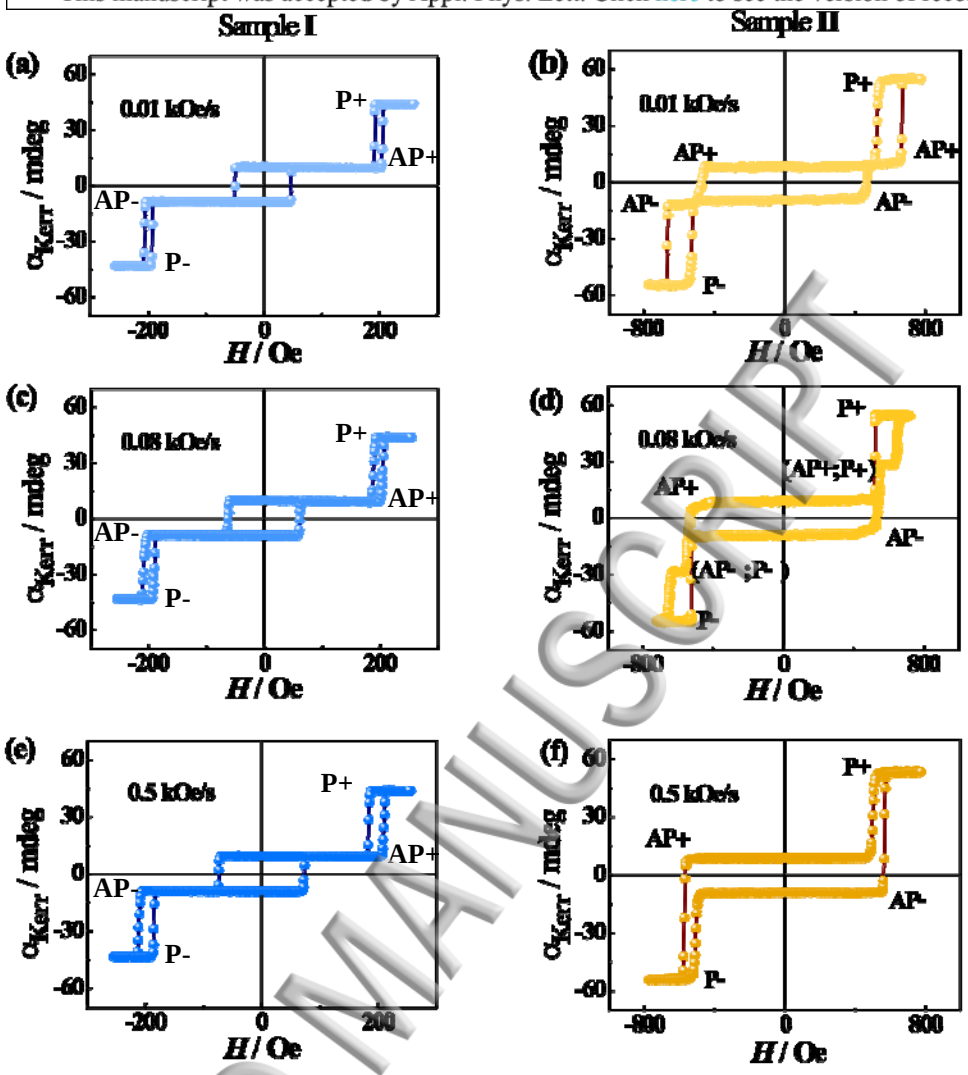

Figure 1.

(a) Sample **I**:

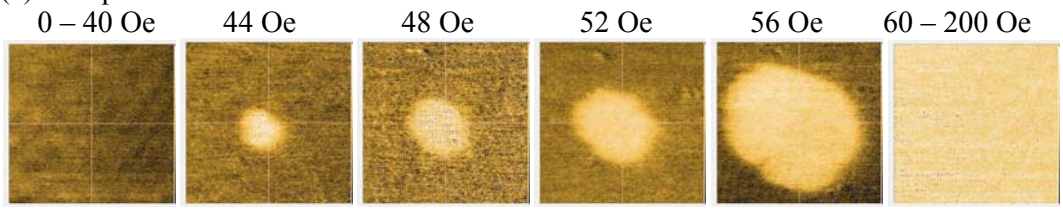

(b) Sample **II**:

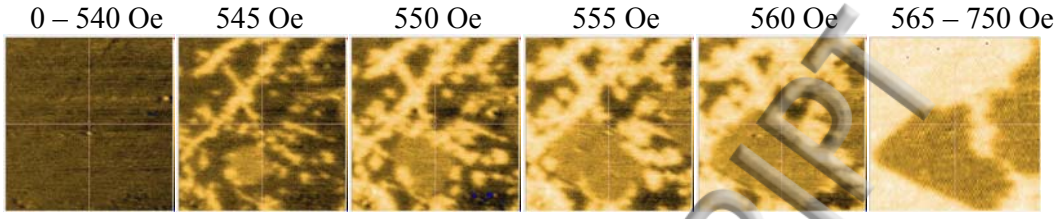

Figure 2.

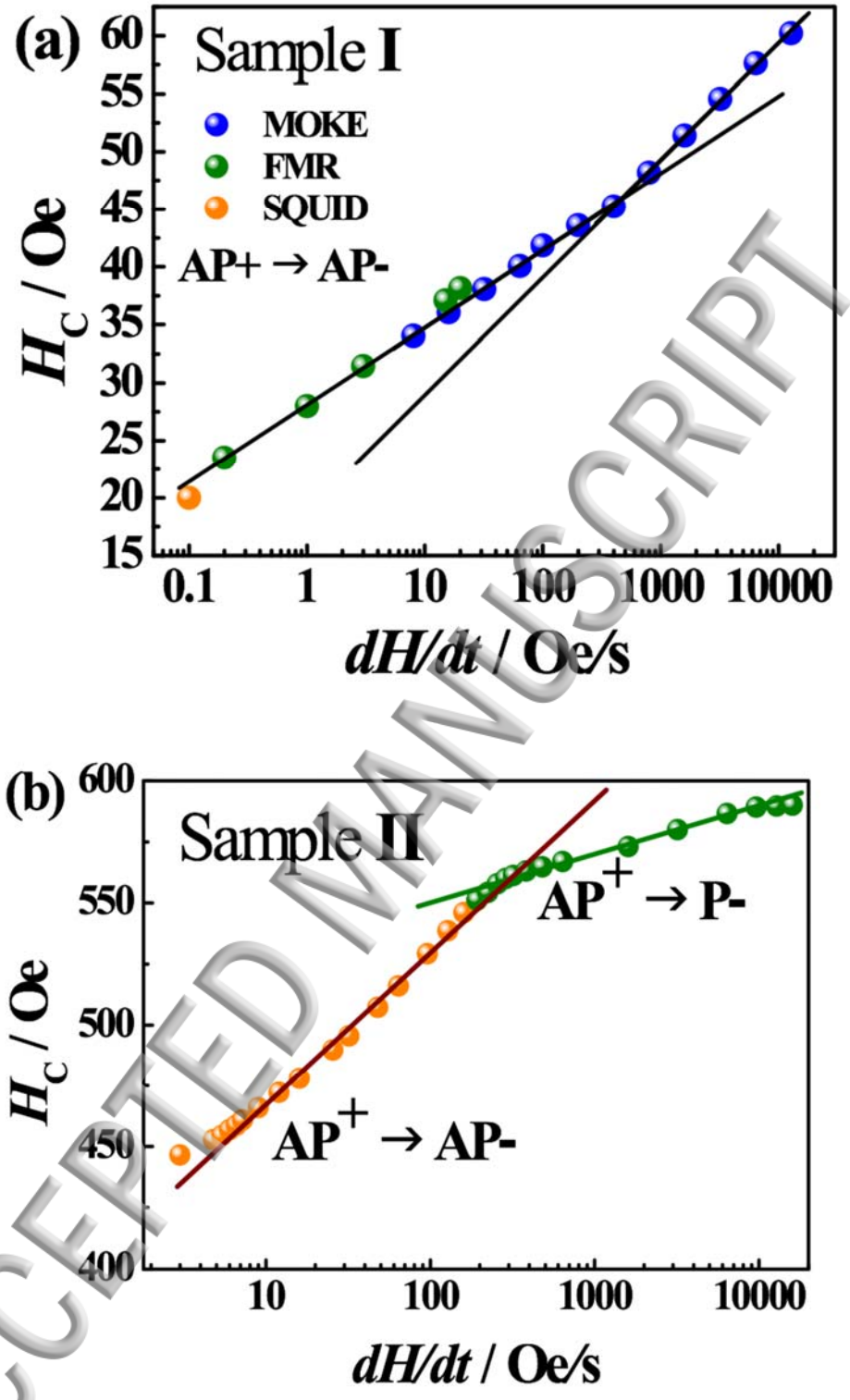

Figure 3.

Sample I

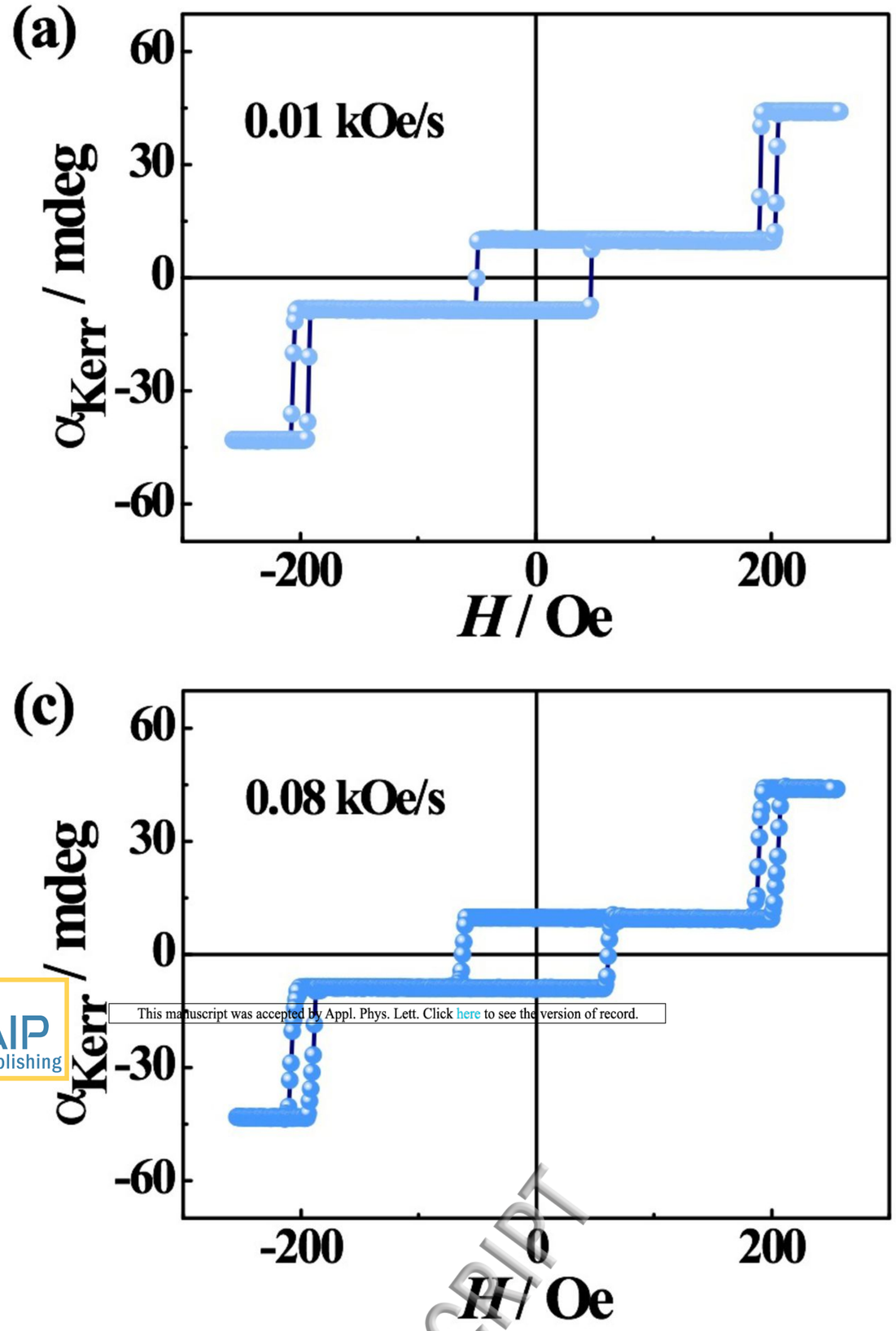

Sample II

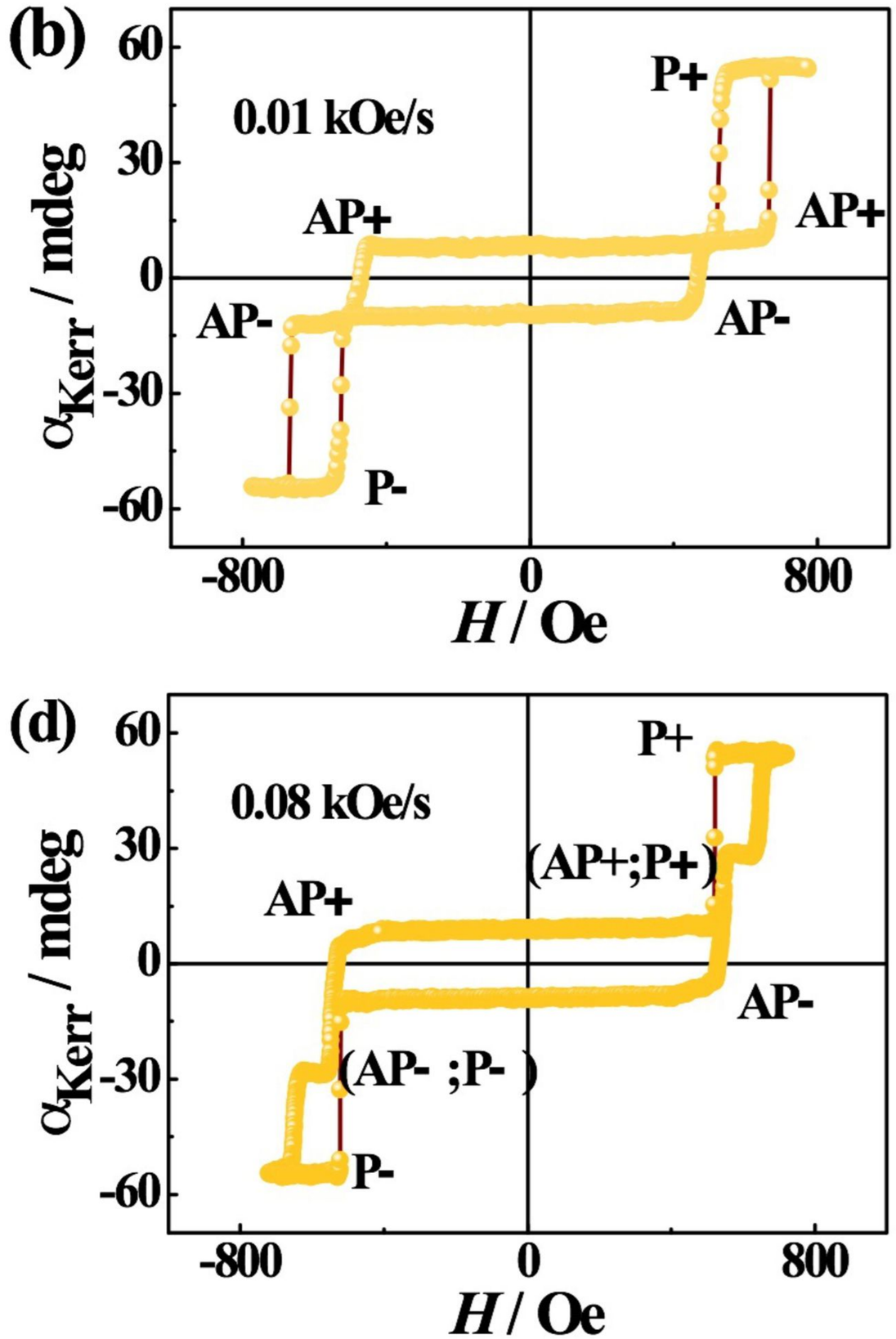

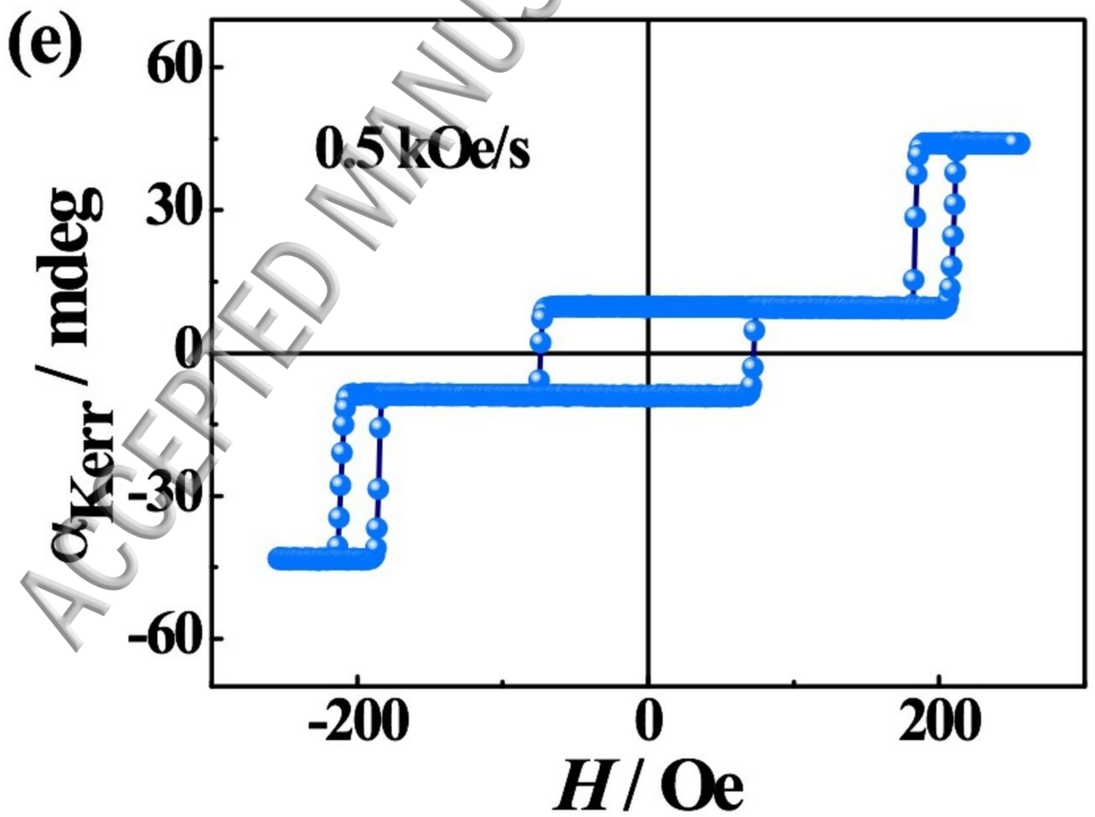

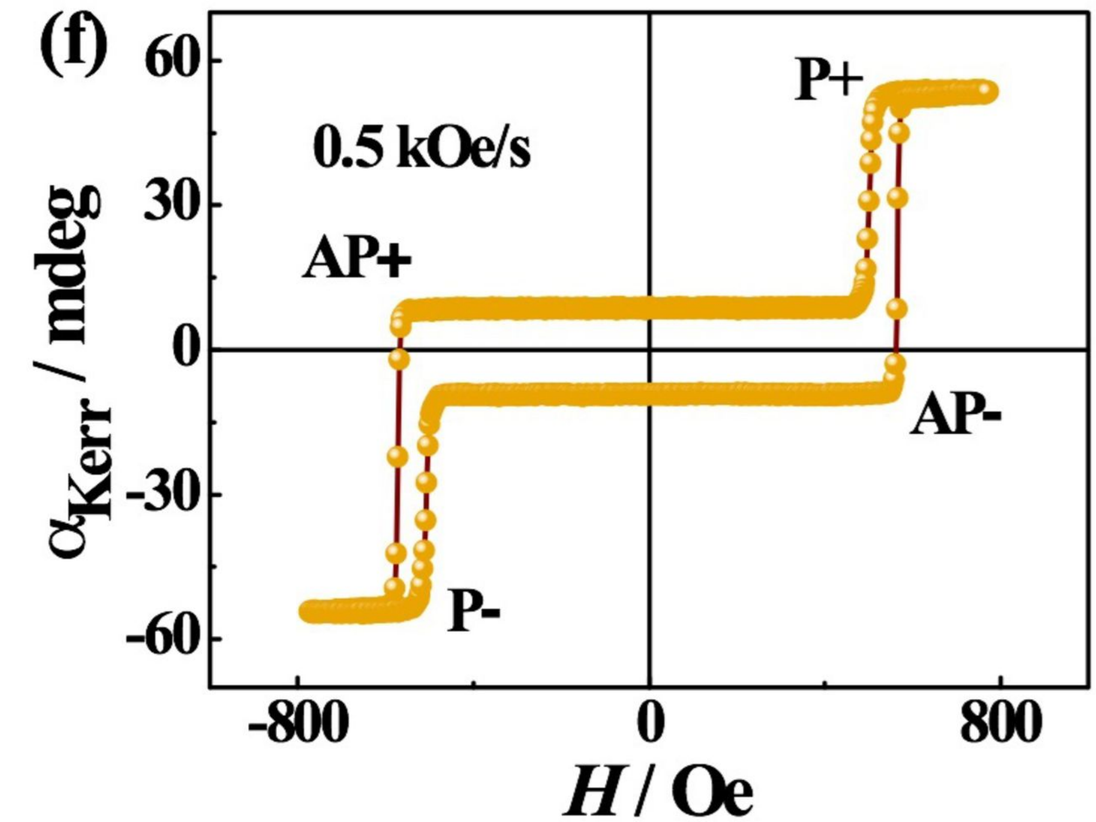

(a) Sample **I**:

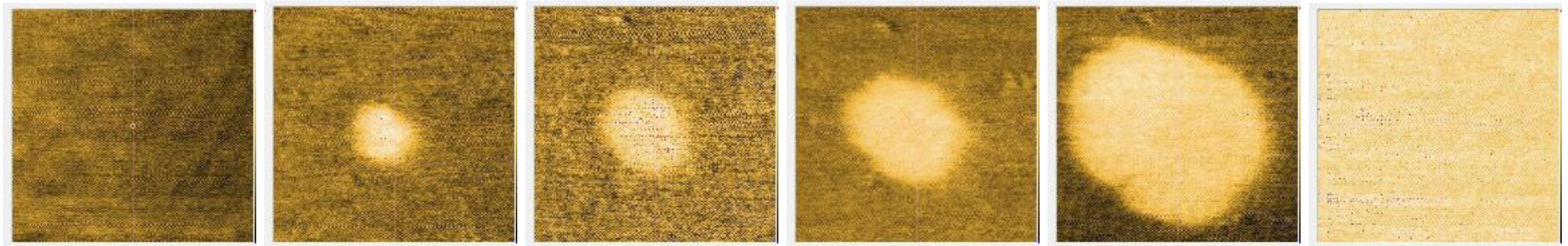

(b) Sample **II**: